27. E. Canales, E. J. Corey, *J. Am. Chem. Soc.* **129**, 12686–12687 (2007).
28. P. Karrer, F. Canal, K. Zohner, R. Widmer, *Helv. Chim. Acta* **11**, 1062–1084 (1928).
29. M. Hajri, C. Blondelle, A. Martinez, J.-L. Vasse, J. Szymoniak, *Tetrahedron Lett.* **54**, 1029–1031 (2013).
30. G. Adamson, A. L. J. Beckwith, M. Kaufmann, A. C. Willis, *J. Chem. Soc. Chem. Commun.* **1995**, 1783–1784 (1995).
31. D. J. Robins, D. S. Rycroft, *Magn. Reson. Chem.* **30**, 1125–1127 (1992).
32. D. Gray, T. Gallagher, *Angew. Chem. Int. Ed.* **45**, 2419–2423 (2006).

Acknowledgments: This work was supported by the Deutsche Forschungsgemeinschaft (Graduiertenkolleg GRK 1626 Chemical Photocatalysis) and by the Fonds der Chemischen Industrie (scholarship to R.B.). We thank O. Ackermann for help in conducting HPLC analyses.

Supplementary Materials
www.sciencemag.org/content/342/6160/840/suppl/DC1
Supplementary Text
Figs. S1 to S8
NMR Spectra
HPLC Spectra
References (*33*–*42*)

16 August 2013; accepted 16 October 2013
10.1126/science.1244809

Abrupt Shifts in Horn of Africa Hydroclimate Since the Last Glacial Maximum

Jessica E. Tierney[1]* and Peter B. deMenocal[2]

The timing and abruptness of the initiation and termination of the Early Holocene African Humid Period are subjects of ongoing debate, with direct consequences for our understanding of abrupt climate change, paleoenvironments, and early human cultural development. Here, we provide proxy evidence from the Horn of Africa region that documents abrupt transitions into and out of the African Humid Period in northeast Africa. Similar and generally synchronous abrupt transitions at other East African sites suggest that rapid shifts in hydroclimate are a regionally coherent feature. Our analysis suggests that the termination of the African Humid Period in the Horn of Africa occurred within centuries, underscoring the nonlinearity of the region's hydroclimate.

During the Early Holocene epoch between roughly 11 to 5 thousand years ago (ka), the presently hyperarid Saharan desert was dotted with large and small lakes, savannah grasslands, and in some regions, humid tropical forests and shrubs (*1*, *2*). This "African Humid Period" (AHP) was a unique hydrological regime and has been a focal point of African paleoclimate studies, both for its climatological implications (*3*, *4*) and its influence on the emergence of pharaonic civilization along the Nile (*5*, *6*). The fundamental cause of the AHP—dramatic increases in summer precipitation triggered by orbital forcing of African monsoonal climate and amplified by oceanic and terrestrial feedbacks—is well understood (*7*, *8*). However, the abruptness with which the AHP began and, most particularly, ended is still debated. Dust proxy data from the west coast of Africa indicate a rapid, century-scale termination of the AHP near 5 ka (*9*). In contrast, isotopic proxies from central Africa (*10*, *11*) and pollen and sedimentological data from a lake in the eastern Sahara (*12*, *13*) suggest a more gradual reduction in rainfall during the mid-Holocene tracking the orbital decline in boreal summer insolation. The discrepancy remains unresolved. Previous studies have attributed the difference in climate response to differing proxy sensitivities; for example, dust may respond nonlinearly to a gradual drying of the Sahara (*14*), and conversely, pollen data may be smoothed because of mixed contributions from distal terrains (*2*). Alternatively, there may be regional heterogeneity in both the timing and duration of the AHP termination, reflecting the variable sensitivity of different regions to certain feedback mechanisms (in particular, vegetation feedbacks) (*3*, *4*, *6*, *15*, *16*).

East Africa and the Arabian Peninsula also experienced humid conditions during the Early Holocene (*17*, *18*). Speleothem $\delta^{18}O$ data from southern Oman (Qunf Cave) and dust strontium isotopes off of Somalia suggest a gradual attenuation of humid conditions during the Holocene, much like the eastern Saharan pollen data (*19*, *20*). These observations have led to the suggestion that the eastern Sahara and northeast Africa experienced a gradual end to the AHP (*3*, *4*, *12*, *15*, *21*) and that abrupt responses were therefore limited to the western Sahara.

We revisited the timing and abruptness of transitions into and out of the AHP in northeast Africa using a new record of hydroclimate from a key, yet previously understudied, region: the Horn of Africa. This record is derived from a marine core (P178-15P) located in the Gulf of Aden (Fig. 1). The Gulf of Aden receives substantial amounts of terrestrial material during the summer monsoon season, when prevailing southwesterly winds transport dust from the Horn (Fig. 1 and fig. S1). Therefore, the terrestrial components (including organic matter) in the sediments predominantly reflect conditions in the Horn and Afar regions (supplementary materials). Twenty radiocarbon dates constrain the chronology of P178-15P and indicate an average sedimentation rate of 32 cm per thousand years (supplementary materials).

We used the hydrogen isotopic composition of leaf waxes (δD_{wax}) as a proxy for aridity and, more generally speaking, hydroclimate, including precipitation/evaporation balance and changes in regional convection. δD_{wax} has been widely used in African paleoclimate and is an effective indicator of changes in the isotopic composition of precipitation (δD_P) and aridity, with enriched isotopic values corresponding to drier conditions and depleted values to wetter conditions (*10*, *22*). More generally, tropical water isotopes are good tracers of large-scale changes in atmospheric circulation (*18*, *23*) and therefore reflect regional, rather than local, shifts in the hydrological cycle. Because Congo basin moisture is effectively blocked by the Ethiopian highlands and the Horn of Africa receives the majority of its rainfall from the Indian Ocean (*24*), we interpret the δD_{wax} values to primarily represent changes in western Indian Ocean hydroclimate.

The δD_{wax} record from the Gulf of Aden indicates that Horn of Africa hydroclimate has changed dramatically during the past 40,000 years (Fig. 2). After the arid conditions of the Last Glacial Maximum (LGM) (26 to 19 ka), the Horn region experienced a severe dry period coincident with the North Atlantic cooling event, Heinrich Event 1 (H1) (Fig. 2), which is consistent with previous proxy (*25*) and model (*23*) evidence

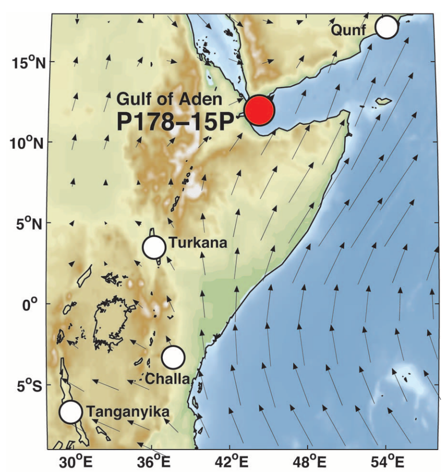

Fig. 1. A map of East Africa. The map includes topography, wind climatology for June-July-August (JJA) (*46*), the location of the study site (Gulf of Aden P178-15P; 11° 57.3′ N, 44° 18′ E, 869 m water depth), and other sites mentioned in the text.

[1]Woods Hole Oceanographic Institution, 266 Woods Hole Road, Woods Hole, MA 02540, USA. [2]Lamont Doherty Earth Observatory, Palisades, NY 10964, USA.

*Corresponding author. E-mail: tierney@whoi.edu

from the Afro-Asian monsoon domain. After H1, there was a rapid transition to intermediate conditions coincident with the Bölling-Allerød (B/A) period and then a reversal into dry conditions during the Younger Dryas (YD), another North Atlantic cold event (Fig. 2). Upon the termination of the YD, the Horn of Africa rapidly moved into the most humid conditions of the past 40,000 years, coincident with the AHP (Fig. 2). These conditions persisted until ~5 ka.

The δD_{wax} record from the Gulf of Aden is dominated by abrupt transitions that occur more rapidly than would be predicted from orbital forcing alone (Fig. 3). Two other δD_{wax} records from East Africa—from Lake Tanganyika (*22*) and Lake Challa (*26*)—show similar and generally coeval abrupt transitions at the end of H1, the YD, and the AHP, even though these sites sit ~2000 km to the south of the Gulf of Aden (Figs. 1 and 3). The overall similarity between the three records attests to the ability of water isotope proxies, specifically δD_{wax}, to record large-scale hydroclimatic patterns in tropical Africa.

The perceived timing and abruptness of the transitions in each δD_{wax} record is subject to dating uncertainties as well as sedimentary properties. Therefore, we used a Monte Carlo method (*27*) to create empirical probability distributions for the midpoint and duration of each identified transition and more clearly assess the duration and synchronicity of these key climate transitions (supplementary materials). We used these distributions to assess the timing of the transitions in a statistical fashion by applying a T test for contemporaneity (*28*) to test against the null hypothesis that the transitions are synchronous between two sites, or a χ^2 test to test against the null hypothesis that the transitions at all three sites derive from the same mean and are therefore likely synchronous. In both cases, we accepted the null hypothesis if $P > 0.05$.

Several findings emerged from this analysis. First, we found that the termination of H1 and the YD are not likely synchronous at all sites. All age model iterations indicate an older timing for the H1–B/A transition at Lake Tanganyika than at the Gulf of Aden site [Lake Challa does not have a detectable H1 termination (supplementary materials)]. The median date of the transition in the Gulf of Aden record [14,680 years before the present (B.P.)] is close to the generally accepted timing of 14,700 years B.P. (*29*), whereas the transition at Lake Tanganyika occurs nearly 1000 years earlier (median = 15,760 years B.P.). For the Challa and Tanganyika sites, the termination of the YD is likely synchronous (t test, P = 0.99) and the timing (median of both = 11,600 years B.P.) is in good agreement with the transition (11,570 years B.P.) dated by tree-ring chronologies (*30*), but the transition in the Gulf of Aden record occurs later in all iterations (median = 10,850 years B.P.).

The observed offsets in the Tanganyika and Aden δD_{wax} data across the H1 and YD terminations, respectively, could reflect meaningful local climatic deviations; however, because these millennial-scale events are remotely forced by North Atlantic processes, it seems more likely that they reflect unconstrained changes in site radiocarbon (^{14}C) reservoirs. Lake Tanganyika has a substantial ^{14}C reservoir today (~1000 years) owing to its meromixis (*22*), and although the evolution of this reservoir is constrained by paired bulk organic matter and terrestrial plant macrofossil dates from the LGM to present (*22*), no data are available for H1, during which time the lake was stratified (*31*). Likewise, we lack sufficient information to constrain how the Gulf of Aden ^{14}C reservoir has evolved through time. Although our site sits outside of the upwelling zone, it is still likely that the regional radiocarbon reservoir was modulated by the intensity of Arabian Sea upwelling, especially during the deglaciation, when large changes

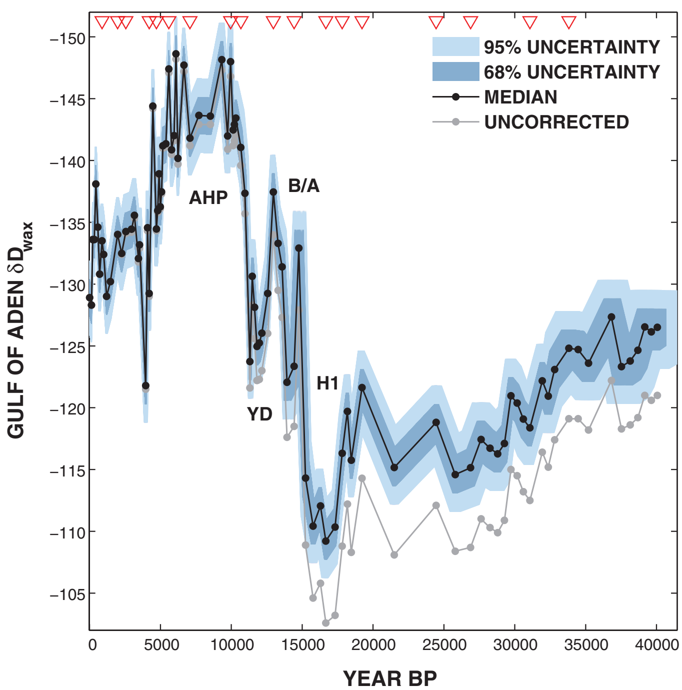

Fig. 2. δD_{wax} data from Gulf of Aden core P178-15P. δD_{wax} data is in per mil versus Vienna standard mean ocean water (VSMOW). Black line denotes median values, with the effect of changing ice volume on the isotopic values removed to isolate the regional hydroclimatic component (supplementary materials). Gray line shows the δD_{wax} data uncorrected for ice volume changes. Shadings indicate empirical 68 and 95% uncertainty bounds (including both analytical- and time-uncertainty) calculated via a Monte Carlo method (*27*). Red triangles denote the stratigraphic locations of radiocarbon dates.

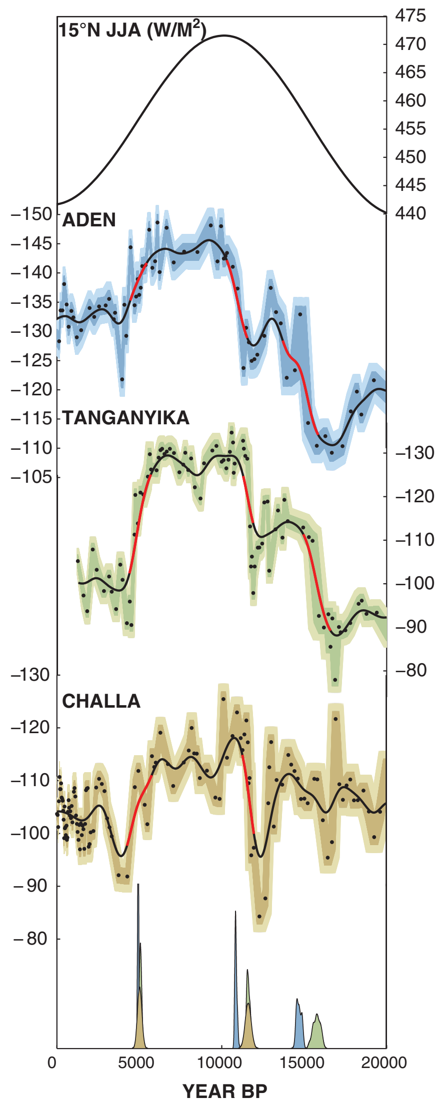

Fig. 3. JJA insolation at 15°N, δD_{wax} data from three sites in East Africa, and the timing of their abrupt transitions. JJA insolation is in watts per square meter, and δD_{wax} data is in per mil versus VSMOW. The effect of changing ice volume on the isotopic values has been removed to isolate the regional hydroclimatic component (supplementary materials). Black markers denote median values, and shadings indicate empirical 68 and 95% uncertainty bounds (including both analytical- and time-uncertainty) calculated via a Monte Carlo method (*27*). Black line indicates the 2000-year Gaussian smoothed time series for each site, with the identified transitions highlighted in red. Probability distributions (bottom) represent the timing of each highlighted transition given the dating uncertainties. Lake Challa δD_{wax} does not indicate a large drying associated with H1 and therefore lacks a H1–B/A transition (supplementary materials).

are known to have occurred and, at least in the eastern Arabian Sea, shifted the ^{14}C reservoir (*32*).

In contrast to the deglacial transitions, our analysis suggests that the termination of the AHP is likely synchronous between all three sites (χ^2 test, $P = 0.25$). Because the mid-Holocene is less likely to be affected by unknown uncertainties in the ^{14}C reservoir (*22*, *32*), we have more confidence that the inferred synchronicity is meaningful. Using Gaussian error reduction, the average timing of the AHP termination from these three East African sites is 4960 ± 70 years B.P. (2σ). This is similar to the revised AHP termination estimate from west Africa of 4900 ± 400 years B.P. (2σ) and is likely synchronous (*t* test, $P = 0.77$).

The observed durations of the identified transitions vary from centuries to millennia (Fig. 4); however, sedimentary factors (sedimentation rates and bioturbation) as well as the sampling rate of the proxy influence how the duration is expressed and attenuated in the time series. As evidence of this, we observed a strong relationship between the duration of the transition and proxy sampling interval (ΔT) [correlation coefficinet (r) = 0.95, $P = 0.0005$] (fig. S2). Normalizing the duration distributions by this sedimentation effect, we arrived at "theoretical" durations representing the most probable duration given a hypothetical infinite sampling rate (Fig. 4). We found that the calculated theoretical durations are short—occurring within centuries—and broadly similar between sites (Fig. 4). The theoretical duration of the termination of the AHP in our Gulf of Aden record ranges from 280 to 490 years. This duration is in accord with a recent analysis of lake level changes in Lake Turkana in northern Kenya: Detailed radiocarbon dating of exposed paleoshoreline horizons revealed that the water level in Lake Turkana dropped permanently by ~50 m within a few centuries at 5270 ± 300 years B.P. (also synchronous with our analyzed timing; *t* test, $P = 0.46$) (*33*). Taken together with our new data from the Gulf of Aden, this suggests that the termination of the AHP was abrupt across a relatively large sector of northeast Africa.

We recognize, however, that there is heterogeneity in terms of the timing and abruptness of the AHP termination across Africa according to the currently available proxy data. Although at low-resolution ($n = 29$ samples; mean ΔT = 470 years), a δD_{wax} record from Lake Victoria has been interpreted as reflecting a gradual termination of the AHP (*34*). Farther to the west, a δD_{wax} record that integrates the Congo drainage basin also shows a gradual termination (*10*), as does a record of the oxygen isotopic composition of seawater from the Gulf of Guinea (*11*). Likewise, to the north of our study site, $\delta^{18}O$ data measured on a Oman stalagmite from Qunf Cave (Fig. 1) suggests a gradual reduction in precipitation across the Arabian Peninsula (*19*). Collectively, these data suggest that abrupt behavior is not a universal feature across Africa and may be restricted to the western Sahara and East Africa.

If this is so, then the feedback mechanisms leading to the observed abrupt shifts may be relatively specific to these regions. In the Sahara and Sahel region, the nonlinear change in rainfall associated with the termination of the AHP likely involves vegetation feedbacks, which enhance the orbitally driven response by changing surface albedo and soil moisture (*35*, *36*). In contrast, vegetation feedbacks are not likely to have occurred within the humid central African zone, where proxy data suggest that vegetation has not shifted substantially (*10*). This may explain the lack of abrupt response in that region. Vegetation feedbacks are also hypothesized to be weaker in the eastern Saharan region because of regional differences in vegetation and soil moisture (*3*, *4*, *15*). In the extreme case, the Arabian Peninsula may not have acquired enough vegetation in the Early Holocene to promote a feedback in spite of more pluvial conditions; limited pollen data suggest a predominance of steppe and grassland but no development of shrubland or dry woodland (*1*, *37*). It is not clear whether vegetation feedbacks universally contributed to the abrupt shifts in East African hydroclimate. Carbon isotopes measured on the same leaf waxes at the sites analyzed here suggest that a vegetation feedback is plausible at Lake Tanganyika, which experienced a dramatic shift from a mixed humid woodland to a more open shrubland (fig. S3). However, there was relatively little shift in the vegetation near Lake Challa and in the Horn of Africa (fig. S3), suggesting that, as with the Arabian Peninsula, a vegetation-driven feedback is unlikely in arid East Africa.

Alternatively, we hypothesize that nonlinear behavior in East African rainfall, including the termination of the AHP, reflects convection feedbacks associated with Indian Ocean sea-surface temperatures (SSTs). This mechanism may explain the difference between the northeast African region and southern Oman. SSTs in the western Indian Ocean hover near the lower bound of the threshold for deep convection (26° to 28°C), and their relationship with deep convection is nonlinear (*38*). Therefore, very small changes in western Indian Ocean SSTs—such as those that occur during Indian Ocean Dipole or El Niño events, as well as oscillations on the multidecadal time scale—can alter the Walker Circulation in the Indian Ocean and induce anomalous deep convection and heavy rainfall in East Africa (*39*, *40*). Rainfall over the southern Arabian Peninsula, although susceptible to such variability (*41*), primarily falls from July through August in association with the Indian summer monsoon, and the influence of the latter likely dominates on orbital time scales (*19*, *21*). Therefore, whereas the gradual trend in the Qunf Cave speleothem record represents the direct response of Arabian hydroclimate to the orbitally driven waning of the boreal summer Indian monsoon, the abrupt shift in East Africa conceivably reflects a convective feedback with a different seasonal dimension. Model simulations suggest that during the Early Holocene, the northward migration of the summer monsoon winds in response to orbital forcing decreased latent heat flux out of the western Indian Ocean, leading to warmer SSTs during the following September-November ("short") rainy season, a reduced east-west SST gradient, and enhanced convection and rainfall over East Africa (*18*, *42*). As the winds migrated south during the Holocene in response to orbital forcing, a critical SST threshold may have been crossed, causing an abrupt cessation of deep convection during the short rainy season and regional aridity. Existing proxy data from the Arabian Sea indicate that Early Holocene SSTs were similar to, or perhaps slightly warmer than, present-day SSTs (*43*, *44*). Meanwhile, eastern Indian Ocean temperatures were slightly cooler (*45*), suggesting a reduced east-west temperature gradient that may have facilitated enhanced convection over East Africa, which is in agreement with the modeling results. It is unclear, however, whether these proxy data are reflecting a change in SSTs during a particular season.

Although further research is needed to investigate the role of Indian Ocean SSTs, the δD_{wax} data presented here suggest that the hydroclimate

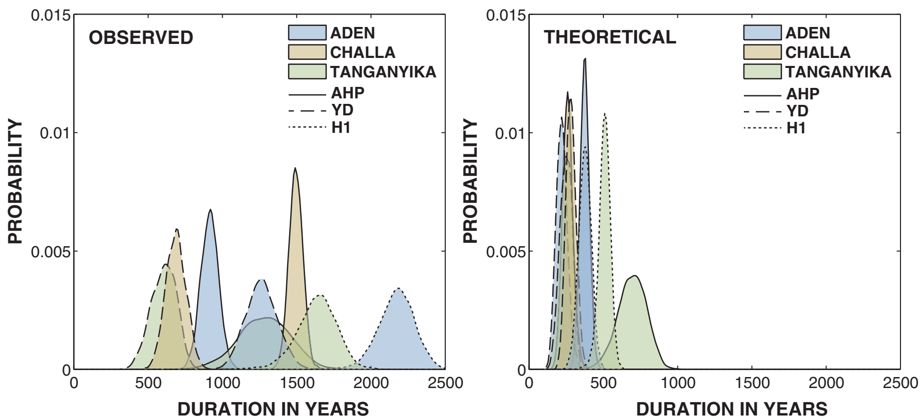

Fig. 4. Observed and theoretical probability distributions. Probability distributions are for the duration of the H1, YD, and AHP terminations at each East African site, corrected for the sampling interval effect (supplementary materials).

of East Africa can rapidly shift from dry and wet conditions. More generally, the Gulf of Aden δD_{wax} record provides a new benchmark of hydroclimatic history for the understudied Horn of Africa region. This study revises our understanding of Holocene climate change in northeast Africa, providing firm evidence that the abrupt termination of the AHP is not limited to the western Sahara. Although the forcings driving the abrupt shifts seen in the paleorecord since the LGM are large and not directly analogous to climate changes experienced today, the possibility of rapid changes in rainfall on human-relevant time scales (centuries) deserves further attention. Paleoclimate data from the past millennium suggest that easternmost Africa was much wetter than present only 300 years ago (*40*), attesting to the dynamic nature of the hydrological cycle in this region. Identifying the mechanisms driving these dramatic and rapid shifts in East African hydroclimate would greatly improve our understanding of the region's climatology, as well as future predictions of food and water security.

References and Notes

1. D. Jolly *et al.*, *J. Biogeogr.* **25**, 1007–1027 (1998).
2. A.-M. Lézine, C. Hély, C. Grenier, P. Braconnot, G. Krinner, *Quat. Sci. Rev.* **30**, 3001–3012 (2011).
3. V. Brovkin, M. Claussen, V. Petoukhov, A. Ganopolski, *J. Geophys. Res.* **103**, 31613 (1998).
4. M. Claussen *et al.*, *Geophys. Res. Lett.* **26**, 2037–2040 (1999).
5. P. Hoelzmann, B. Keding, H. Berke, S. Kröpelin, H.-J. Kruse, *Palaeogeogr. Palaeoclimatol. Palaeoecol.* **169**, 193–217 (2001).
6. R. Kuper, S. Kröpelin, *Science* **313**, 803–807 (2006).
7. J. E. Kutzbach, B. L. Otto-Bliesner, *J. Atmos. Sci.* **39**, 1177–1188 (1982).
8. M. Claussen, V. Gayler, *Global Ecol. Biogeo. Lett.* **6**, 369–377 (1997).
9. P. B. deMenocal *et al.*, *Quat. Sci. Rev.* **19**, 347–361 (2000).
10. E. Schefuß, S. Schouten, R. R. Schneider, *Nature* **437**, 1003–1006 (2005).
11. S. Weldeab, D. W. Lea, R. R. Schneider, N. Andersen, *Science* **316**, 1303–1307 (2007).
12. S. Kröpelin *et al.*, *Science* **320**, 765–768 (2008).
13. P. Francus *et al.*, *Sedimentology* **60**, 911–934 (2013).
14. J. A. Holmes, *Science* **320**, 752–753 (2008).
15. V. Brovkin, M. Claussen, *Science* **322**, 1326b (2008).
16. S. Bathiany, M. Claussen, K. Fraedrich, *Clim. Dyn.* **38**, 1775–1790 (2012).
17. F. A. Street-Perrott, D. S. Marchand, N. Roberts, S. P. Harrison, *U.S. Department of Energy Technical Report* 46 (U.S. Department of Energy Washington, DC, 1989).
18. J. E. Tierney, S. C. Lewis, B. I. Cook, A. N. LeGrande, G. A. Schmidt, *Earth Planet. Sci. Lett.* **307**, 103–112 (2011).
19. D. Fleitmann *et al.*, *Science* **300**, 1737–1739 (2003).
20. S. Jung, G. Davies, G. Ganssen, D. Kroon, *Earth Planet. Sci. Lett.* **221**, 27–37 (2004).
21. D. Fleitmann *et al.*, *Quat. Sci. Rev.* **26**, 170–188 (2007).
22. J. E. Tierney *et al.*, *Science* **322**, 252–255 (2008).
23. F. Pausata, D. Battisti, K. Nisancioglu, C. Bitz, *Nat. Geosci.* **4**, 474–480 (2011).
24. J. Slingo, H. Spencer, B. Hoskins, P. Berrisford, E. Black, *Philos. Trans. A Math. Phys. Eng. Sci.* **363**, 25–42 (2005).
25. J. C. Stager, D. B. Ryves, B. M. Chase, F. S. Pausata, *Science* **331**, 1299–1302 (2011).
26. J. E. Tierney, J. M. Russell, J. S. Sinninghe Damsté, Y. Huang, D. Verschuren, *Quat. Sci. Rev.* **30**, 798–807 (2011).
27. K. J. Anchukaitis, J. E. Tierney, *Clim. Dyn.* **41**, 1291–1306 (2013).
28. A. Long, B. Rippeteau, *Am. Antiq.* **39**, 205 (1974).
29. K. A. Hughen, T. I. Eglinton, L. Xu, M. C. Makou, *Science* **304**, 1955–1959 (2004).
30. M. Friedrich, B. Kromer, M. Spurk, J. Hofmann, K. Felix Kaiser, *Quat. Int.* **61**, 27–39 (1999).
31. J. E. Tierney, J. M. Russell, *Geophys. Res. Lett.* **34**, L15709 (2007).
32. M. Staubwasser, F. Sirocko, P. M. Grootes, H. Erlenkeuser, *Paleoceanography* **17**, 15-1–15-2 (2002).
33. Y. Garcin, D. Melnick, M. R. Strecker, D. Olago, J.-J. Tiercelin, *Earth Planet. Sci. Lett.* **331**, 322–334 (2012).
34. M. A. Berke *et al.*, *Quat. Sci. Rev.* **55**, 59–74 (2012).
35. J. G. Charney, *Q. J. R. Meteorol. Soc.* **101**, 193–202 (1975).
36. J. Shukla, Y. Mintz, *Science* **215**, 1498–1501 (1982).
37. A. Parker *et al.*, *J. Quaternary Sci.* **19**, 665–676 (2004).
38. C. Zhang, *J. Clim.* **6**, 1898–1913 (1993).
39. E. Black, J. Slingo, K. R. Sperber, *Mon. Weather Rev.* **131**, 74–94 (2003).
40. J. E. Tierney, J. E. Smerdon, K. J. Anchukaitis, R. Seager, *Nature* **493**, 389–392 (2013).
41. A. Chakraborty, S. K. Behera, M. Mujumdar, R. Ohba, T. Yamagata, *Mon. Weather Rev.* **134**, 598–617 (2006).
42. Y. Zhao *et al.*, *Clim. Dyn.* **25**, 777–800 (2005).
43. F. Rostek, E. Bard, L. Beaufort, C. Sonzogni, G. Ganssen, *Deep Sea Res. Part II Top. Stud. Oceanogr.* **44**, 1461–1480 (1997).
44. P. Anand *et al.*, *Paleoceanography* **23**, PA4207 (2008).
45. M. Mohtadi, S. Steinke, A. Lückge, J. Groeneveld, E. Hathorne, *Earth Planet. Sci. Lett.* **292**, 89–97 (2010).
46. E. Kalnay *et al.*, *Bull. Am. Meteorol. Soc.* **77**, 437–471 (1996).

Acknowledgments: This study was supported by National Science Foundation grant OCE-1203892 to J.E.T., National Oceanic and Atmospheric Administration award NAO80AR4320912 to P.B.d.M., and the Lamont-Doherty Earth Observatory (LDEO) Climate and Life Initiative. We thank E. Hamilton and C. Johnson for assistance with the stable isotope measurements; J.-B. Stuut, G. Ganssen, and C. Cleroux for assistance with core sampling; J. Fang and T. Guilderson for assistance with the radiocarbon dating; and C. Ummenhofer for comments on the initial versions of the manuscript. We thank the Captain and crew of the *R/V Pelagia* for their remarkable professionalism during the penultimate leg (Cruise 178; April to May 2001) of the scientific circumnavigation of the African continent. With co-chief scientist G. Ganssen, we were able to obtain valuable samples from this remote and geopolitically challenging region. This is LDEO contribution number 7739.

Supplementary Materials
www.sciencemag.org/content/342/6160/843/suppl/DC1
Materials and Methods
Figs. S1 to S3
Tables S1 and S2
References

13 May 2013; accepted 26 September 2013
Published online 10 October 2013;
10.1126/science.1240411

Dosage Compensation via Transposable Element Mediated Rewiring of a Regulatory Network

Christopher E. Ellison and Doris Bachtrog*

Transposable elements (TEs) may contribute to evolutionary innovations through the rewiring of networks by supplying ready-to-use cis regulatory elements. Genes on the *Drosophila* X chromosome are coordinately regulated by the male specific lethal (MSL) complex to achieve dosage compensation in males. We show that the acquisition of dozens of MSL binding sites on evolutionarily new X chromosomes was facilitated by the independent co-option of a mutant helitron TE that attracts the MSL complex (TE domestication). The recently formed neo-X recruits helitrons that provide dozens of functional, but suboptimal, MSL binding sites, whereas the older XR chromosome has ceased acquisition and appears to have fine-tuned the binding affinities of more ancient elements for the MSL complex. Thus, TE-mediated rewiring of regulatory networks through domestication and amplification may be followed by fine-tuning of the cis-regulatory element supplied by the TE and erosion of nonfunctional regions.

Active transposable elements (TEs) impose a substantial mutational burden on the host genome (*1–4*). However, there is growing evidence implicating TEs as drivers of key evolutionary innovations by creating or rewiring regulatory networks (*5–11*). Many TEs harbor a variety of regulatory motifs, and TE amplification may allow for the rapid accumulation of a specific motif throughout the genome, thus recruiting multiple genes into a single regulatory network (*12*).

In *Drosophila miranda*, multiple sex chromosome/autosome fusions have created a series of X chromosomes of differing ages (Fig. 1). The ancestral X chromosome, XL, is homologous to the *D. melanogaster* X and is at least 60 million years old (*13*). Chromosome XR became a sex chromosome ~15 million years ago and is shared among members of the *affinis* and *pseudoobscura* subgroups, whereas the neo-X chromosome is specific to *D. miranda* and originated only 1 million years ago (*14*, *15*). The male specific lethal (MSL) complex coordinates gene expression on the *Drosophila* male X to achieve dosage compensation (*16*). This complex is recruited to the X chromosome in males to high-affinity chromatin entry sites (CES) containing a conserved, roughly 21–base

Department of Integrative Biology, University of California, Berkeley, Berkeley, CA 94720, USA.

*Corresponding author. E-mail: dbachtrog@berkeley.edu